PAN
ARCHIVES OF ACOUSTICS
Vol. **44**, No. 3, pp. 521–531 (2019)
DOI: 10.24425/aoa.2019.129267

Performance Evaluation of T-Shaped Noise Barriers Covered with Oblique Diffusers Using Boundary Element Method

Mohammad Reza MONAZZAM[1], Milad ABBASI[2], Saeid YAZDANIRAD[3],[4]*

[1] *Department of Occupational Health Engineering*
School of Public Health
Tehran University of Medical Sciences
Tehran, Iran; e-mail: mmonazzam@hotmail.com

[2] *Research Center for Environmental Determinants of Health (RCEDH)*
Health Institute, Kermanshah University of Medical Sciences
Kermanshah, Iran; e-mail: milad8285@gmail.com

[3] *School of Health*
Shahrekord University of Medical Sciences
Shahrekord, Iran
*Corresponding Author e-mail: saeedyazdanirad@gmail.com

[4] *Students' Scientific Research Center*
Tehran University of Medical Sciences
Tehran, Iran

(*received March 9, 2018; accepted March 9, 2019*)

One of the most effective designs to control the road traffic noise is the T-shaped barrier. The aim of this study was to examine the performance of T-shape noise barriers covered with oblique diffusers using boundary element method. A 2D simulation technique based on the boundary element method (BEM) was used to compute the insertion loss at the center frequency of each one-third octave band. In designed barriers, the top surface of the T-shaped noise barriers was covered with oblique diffusers. The width and height of the barrier stem and the width of its cap were 0.3, 2.7, and 1 m, respectively. Angles of the oblique diffusers were 15, 30, and 45 degrees. The oblique diffusers were placed on the top surface with two designs including same oblique diffusers (SOD) and quadratic residue oblique diffusers (QROD). Barriers considered were made of concrete, an acoustically rigid material. The barrier with characteristics of QROD, forward direction, and sequence of angles (15, 30, and 45 degrees) had the greatest value of the overall A-weighted insertion loss equal to 18.3 to 21.8 dBA at a distance of 20 m with various heights of 0 to 6 m.

Keywords: noise barrier; oblique diffuser; T-shaped; boundary element method.

1. Introduction

In recent years, growing urbanization and increased numbers of vehicles have resulted in traffic noise level above permissible values. The adverse effects of exposure to traffic noise for residents of the roadside areas are well-known including cardiovascular disease, digestive disorders, sleep disturbance, and impacts on cognitive performance (Basner *et al.*, 2014; Abbasi *et al.*, 2015; Khoshakhlagh *et al.*, 2017). There are a few techniques for decreasing the road traffic noise. Standards such as EN 1793-3 and EN 1793-4 have been developed that recommend test methods for determining the acoustic performance of the road traffic noise-reducing devices (Garai, 2004; EN No: 1793-4, 2015). These standards also apply to the development of effective added devices for road traffic noise barriers (Garai, Guidorzi, 2007). Noise barriers are one of the most effective methods for environmental noise control. In general, a barrier reduces the sound waves transmitted to a receiver in the shadow area, shielding the direct path. The receiver may receive the noise

by other indirect paths such as refraction on the barrier top.

Numerous studies have been carried out to explore enhancement of noise barrier efficiency. These studies can be categorized into several groups based on the variations including dimension, location, material, shape, and use of absorbent materials at the barriers (Yamamoto, 2015). Initially, researchers tried to improve efficiency by changing the dimensions and location of barriers. Hothersall *et al.* (1991) noted that an increased height of 3 to 5 m can improve the insertion loss by 3.8 dB. May and Osman (1980) introduced the wide top barriers and concluded a barrier with a cap width of 2.44 m increases the efficiency by 3.1 dB. However, the dimensional variations may cause secondary problems such as reduced sunlight, altered aesthetics and high cost. Some researchers have studied the materials used in barriers. Halim *et al.* (2015) examined the effectiveness of noise barriers made of vegetation, concrete hollow block, and panel concrete. The results revealed that panel concrete provides an insertion loss greater than that of the concrete hollow block and vegetation. A study conducted by Koussa *et al.* (2013) on the acoustic performance of low height gabions noise barriers indicated that the insertion loss values can reach 8 dBA at the shadow zone. Another group of researchers demonstrated that the barrier top causes noise refraction and decreases performance. They applied an absorptive material on the top edge of a barrier (Okubo *et al.*, 2010). As the practical use of absorbent materials in barriers was difficult, researchers changed the shape of the barrier top and designed various shapes of barriers such as T-shape, Y-shape, arrow-shaped, cylinder and thnadner to increase its efficiency (Fard *et al.*, 2013). Wang *et al.* (2018) examined the effect of wells mounted on the top edge of the barrier. Results showed that wells increase the insertion loss by 1.5 dBA. Greiner *et al.* (2010) also conducted a study to achieve an optimum design of the Y-shaped barrier using the multi-objective evolutionary algorithm. The suggested methodology improved the IL spectrum of the Y-shaped barrier by 15% and 30%. Of various barrier types, one of the most effective designs is the T-shaped barrier. As found by Ishizuka and Fujiwara, the soft T-shaped barrier exhibits the highest performance among noise barriers with various edge shapes. A T-shaped barrier with 3-m height performs as well as a plain one with 10-m height (Ishizuka, Fujiwara, 2004). Hothersall *et al.* reviewed results of previous researches on the insertion loss of T-, Y- and arrow-shaped noise barriers. Results revealed that Y- and arrow-shaped barriers were less efficient than T-shaped ones (Hothersall *et al.*, 1991).

Some researchers used diffusers on top surface of the barrier to increase its performance. Baulac *et al.* (2008) optimized the acoustical efficiency of T-shaped noise barriers covered with a series of wells using the generic algorithm and the results showed that the efficiency can be improved 2–3 dBA for 5–9 wells. Monazzam *et al.* (2010) employed the primitive root sequence diffuser (PRD) on a T-shaped barrier design. Insertion loss of the designed barrier improved nearly 2 to 3 dB compared to its equivalent rigid barrier at far field. In addition, Fan *et al.* (2013) used an active control system at T-shaped barrier and achieved an extra insertion loss of more than 3 dBA. Oblique surfaces can also be used to reflect and diffuse sound. There is a patent that covers the use of these surfaces on the face of barriers (McNair, 1995). In the present study, various types of oblique diffusers on the top surface of T-shaped barrier were applied for improvement of its performance. Therefore, the aim of this study was to examine the performance of T-shape noise barriers covered with oblique diffusers using boundary element method.

2. Materials and methods

2.1. Boundary element method

In the current study, a two-dimensional simulation technique, based on the boundary element method (BEM), was used to compute the insertion loss. In this method, the surface conditions can be calculated. The advantage is the accuracy and flexibility in representation of the different shapes. BEM is a strong instrument for the assessment of the acoustic performance of various noise barriers. Numerous studies have successfully applied this method for determining the effectiveness of noise barriers (Greiner *et al.*, 2010; Monazzam *et al.*, 2010). The method allows a precise assessment of the acoustic pressure field around noise barriers with different shapes, and provides an opportunity for investigation and comparison of various barriers (Naderzadeh *et al.*, 2011).

BEM has two axis included the horizontal axis (x) on the ground plane and the vertical axis (y) which is perpendicular to the ground plane. A steady line source is at $r_0 = (x_0, y_0)$ and the acoustic pressure ($p(r, r_0)$) is at $r = (x, y)$. BEM divides the surface of the barrier into a number of line elements (γ_1, γ_2, ..., γ_n) and calculates the Helmholtz equation for each element. The dimension of elements is less than one-fifth of a wavelength and it is assumed that $p(r_0, r_n)$ is constant for each element (Hothersall *et al.*, 1991). Then, BEM solves the Helmholtz wave equation at a frequency (Brunner *et al.*, 2010):

$$\varepsilon(r)p(r,r_0) = G(r,r_0) + \int_{\gamma}\left(\frac{\partial G(r_s,r)}{\partial n(r_s)} - ik\beta(r_s)G(r_s,r)\right) \cdot p(r_s,r_0)\partial s(r_s), \tag{1}$$

where $\partial s(r_s)$ is the length of an element of γ at r_s and $\frac{\partial}{\partial n(r_s)}$ is the normal derivative at r_s; k also shows the wave number. As well as, on a rigid ground, $G(r, r_0)$ indicates the acoustic pressure at r of a source at r_0 and could be calculated as:

$$G(r, r_0) = -\frac{i}{4}\left\{H_0^{(1)}\left(k\left|r_0 - r\right|\right) + H_0^{(1)}\left(k\left|r_0' - r\right|\right)\right\}, \quad (2)$$

where r_0' is the image of the source on the ground ($r_0' = (x_0 - y_0)$) and $H_0^{(1)}$ shows the Hankel function of the first kind of zero order.

However, in BEM, turbulence and degradation due to temperature, humidity and other climatic conditions are not considered. The above calculations were solved in FORTRAN. More details are described in the Monazzam and Lam (2005) study. The comparison of this model with experimental results shows an acceptable correlation at the wide range of frequencies (Monazzam, Lam, 2008).

2.2. Performance evaluation

In the current study, the insertion loss was calculated by the Eq. (3) at the center frequency of each one-third octave band to evaluate the performance.

$$IL = -20\log_{10}\left|\frac{p\left(r, r_0\right)}{G\left(r, r_0\right)}\right| \quad [\text{dB}], \quad (3)$$

where $p\left(r, r_0\right)$ and $G\left(r, r_0\right)$ are the sound pressure with and without acoustic barriers at the receiver point, respectively. As well as, the overall A-weighted insertion loss (IL_A) was calculated based on the BS EN 1793-3:1998 standard using Eq. (4) to combine the results of the insertion loss at the center frequencies of the one-third octave band over the range 100–4000 Hz (EN 1793-3, 1998).

$$IL_{\text{total}} = -10\log\left(\frac{\sum\left(10^{0.1(L_i+8)}\cdot 10^{-0.1IL_i}\right)}{\sum\frac{E_{w/oi}}{E_{1\text{ kHz}}}}\right), \quad (4)$$

where the values of L_i are extracted from Table 1 and normalized to 1 kHz, IL_i represents the insertion loss at f_i as frequency, $E_{w/oi}$ and $E_{1\text{ kHz}}$ are the sound energy on the flat ground without barrier at different frequencies and 1 kHz, respectively.

2.3. Specifications of designed noise barriers

Figure 1 illustrates various designed noise barriers and Table 2 describes their characteristics. The first barrier is a reference T-shaped rigid barrier with variations performed on it. The width and height of the barrier stem and the length and width of the cap were 0.3, 2.7, 1, and 0.3 m, respectively. In designed barriers, the top surface of the T-shaped barrier was covered with oblique diffusers. The width and height of their stems and the length of their caps were approximately similar to those of the reference T-shaped barrier. Three oblique diffusers were used in the barriers. Angles of oblique diffusers were 15, 30, and 45 degrees. Oblique diffusers were placed on the top surface

Table 1. Normalized traffic noise spectrum.

f_i [Hz]	L_i [dB]
100	−20
125	−20
160	−18
200	−16
250	−15
315	−14
400	−13
500	−12
630	−11
800	−9
1000	−8
1250	−9
1600	−10
2000	−11
2500	−13
3150	−15
4000	−16

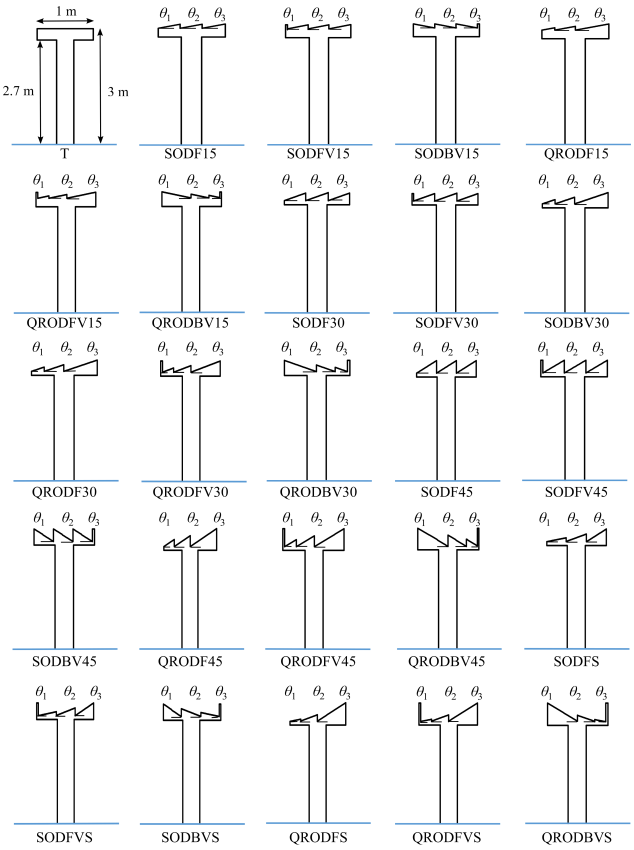

Fig. 1. The various designed noise barriers.

Table 2. The characteristics of various designed noise barriers.

Model	Characteristics					
	θ_1 [deg]	θ_2 [deg]	θ_3 [deg]	The width of the barrier stem [m]	The height of the barrier stem [m]	The length of the barrier cap [m]
T	0	0	0	0.3	2.7	1
SODF15	15	15	15	0.3	2.7	0.99
SODFV15	15	15	15	0.3	2.7	1.02
SODBV15	15	15	15	0.3	2.7	1
QRODF15	15	15	15	0.3	2.7	0.99
QRODFV15	15	15	15	0.3	2.7	1.02
QRODBV15	15	15	15	0.3	2.7	1.01
SODF30	30	30	30	0.3	2.7	1
SODFV30	30	30	30	0.3	2.7	1.03
SODBV30	30	30	30	0.3	2.7	1.03
QRODF30	30	30	30	0.3	2.7	0.99
QRODFV30	30	30	30	0.3	2.7	1.02
QRODBV30	30	30	30	0.3	2.7	1.01
SODF45	45	45	45	0.3	2.7	0.99
SODFV45	45	45	45	0.3	2.7	1.02
SODBV45	45	45	45	0.3	2.7	0.99
QRODF45	45	45	45	0.3	2.7	0.99
QRODFV45	45	45	45	0.3	2.7	1.02
QRODBV45	45	45	45	0.3	2.7	1
SODFS	15	30	45	0.3	2.7	0.99
SODFVS	15	30	45	0.3	2.7	1.02
SODBVS	45	30	15	0.3	2.7	1.01
QRODFS	15	30	45	0.3	2.7	0.99
QRODFVS	15	30	45	0.3	2.7	1.02
QRODBVS	45	30	15	0.3	2.7	1

based on two designs including the base size of triangles with equal sequences as same oblique diffusers (SOD) and with quadratic residue sequences (Sequence: 2 3 5) as quadratic residue oblique diffusers (QROD). In addition, the direction of diffusers linked to the sound source were forward and backward. In some oblique barriers, the vertical edge was used at the end of the barrier for the wave. Barriers were made of concrete, which is an acoustically rigid material.

2.4. Parameters for calculation

The sound source was located at a distance of 5 meters from the center line of barriers on rigid ground to simulate the mean distance of vehicles on a normal highway. In addition, the receiver point was placed at a distance of 20 meters from the center line of the barriers with the various heights (0, 1.5, 3, 4.5 and 6 meters) of the rigid ground. All calculations were performed at the center frequencies of the third-octave band over the range 100–4000 Hz. In general, the efficiency of each designed barrier was compared to that of the reference T-shaped barrier. In the next step, the designed barrier with the best performance was selected for subsequent calculations. The overall A-weighted insertion loss of the barrier with the best performance and reference T-shaped one were calculated at different distances from the barrier (5, 20, 50, and 100 meters) and heights of 0, 1.5, 3, 4.5, and 6 meters above the ground. Figure 2 depicts the locations of the various receiver points at the shadow zone.

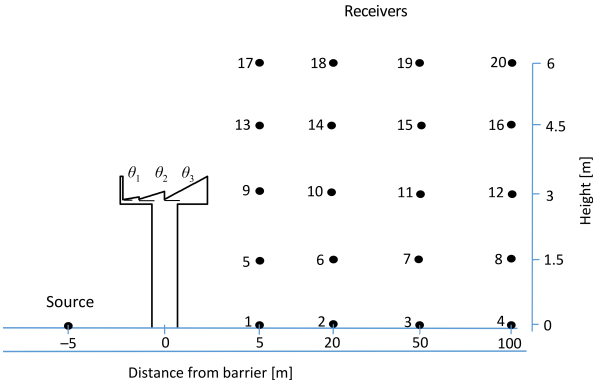

Fig. 2. The locations of various receiver points at the shadow zone.

3. Results

Figures 3, 4, 5, 6, and 7 indicate the overall A-weighted insertion loss [dBA] in barriers designed by oblique diffusers compared to that of in the reference T-shaped barrier at a distance of 20 meters and heights of 0, 1.5, 3, 4.5, and 6 meters. Based on the results, some barrier models including SODFV1 and SODBV15 had the overall A-weighted insertion loss less than that of the reference T-shaped barrier at some heights. Other barriers have a better performance relative to T-shaped barriers at various heights. However, barrier model of QRODFVS compared to the reference T-shaped barrier had the best performance at various heights. Other barrier models showed very different performance at various heights.

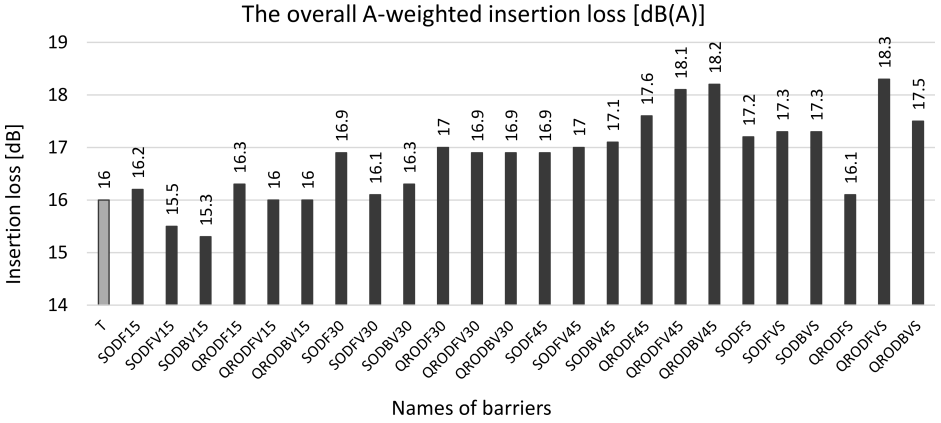

Fig. 3. The overall A-weighted insertion loss [dBA] in barriers designed by oblique diffusers compared to that of in the reference T-shaped barrier at the receiver point (20, 0).

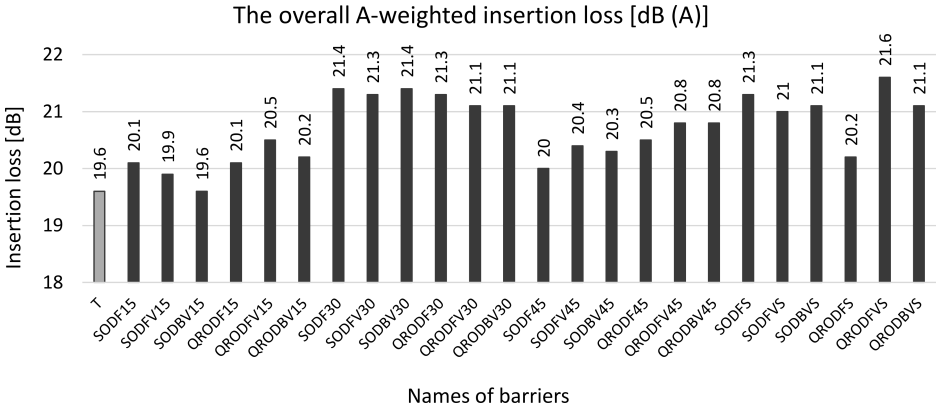

Fig. 4. The overall A-weighted insertion loss [dBA] in barriers designed by oblique diffusers compared to that of in the reference T-shaped barrier at the receiver point (20, 1.5).

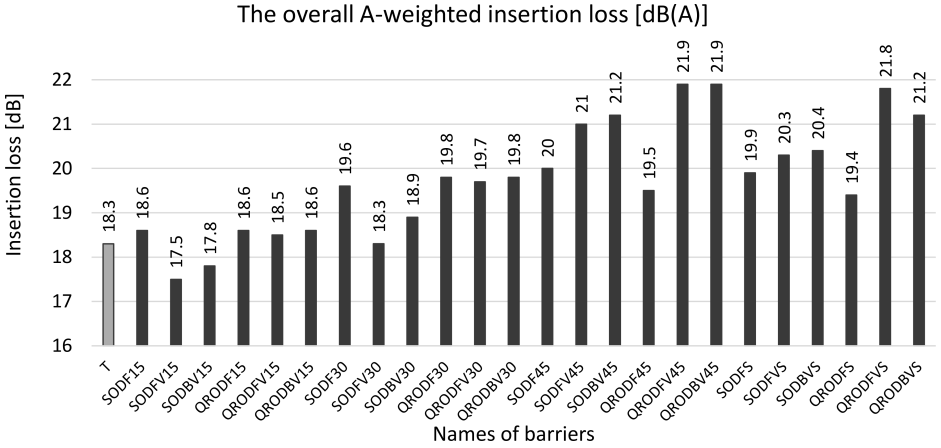

Fig. 5. The overall A-weighted insertion loss [dBA] in barriers designed by oblique diffusers compared to that of in the reference T-shaped barrier at the receiver point (20, 3).

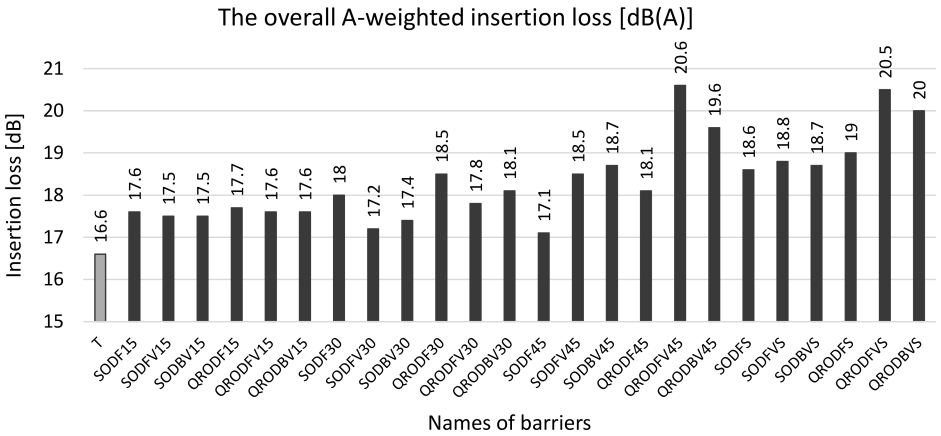

Fig. 6. The overall A-weighted insertion loss [dBA] in barriers designed by oblique diffusers compared to that of in the reference T-shaped barrier at the receiver point (20, 4.5).

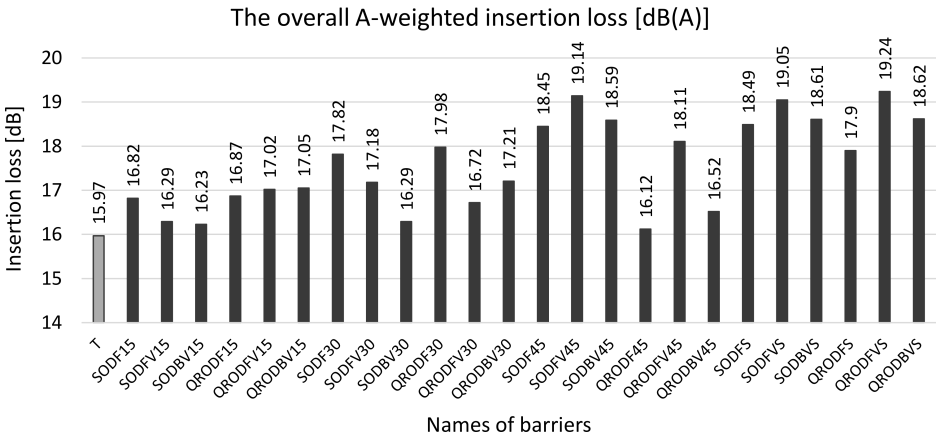

Fig. 7. The overall A-weighted insertion loss [dBA] in barriers designed by oblique diffusers compared to that of in the reference T-shaped barrier at the receiver point (20, 6).

Figures 8, 9, 10, 11, and 12 illustrate the Predicted frequency spectra of the barrier insertion loss [dBA] for T-shaped and QRODFVS barriers at different heights for a distance of 20 m. Values of the insertion loss in the QRODFVS barrier compared to the reference T-shaped barrier had no significant difference at frequencies less than 200 Hz. Changes in the values of the insertion loss have been often made at frequencies more than 200 Hz. The frequency with the best performance for various designed barriers at various heights

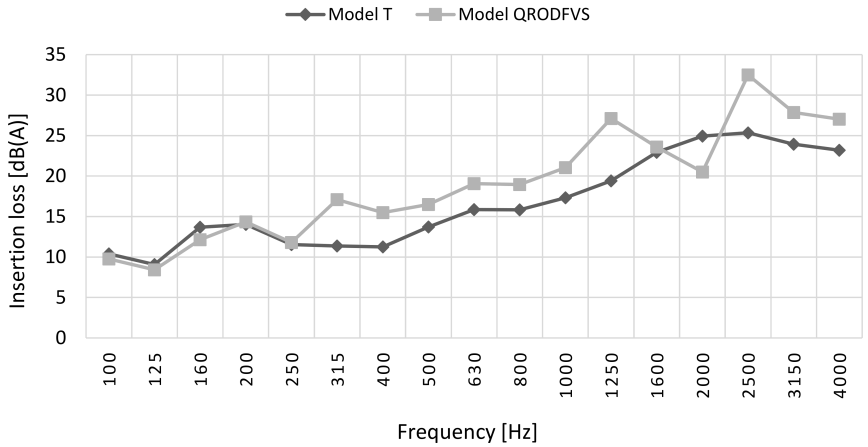

Fig. 8. The Predicted frequency spectra of the barrier insertion loss [dBA] for T-shaped and QRODFVS at the receiver point (20, 0).

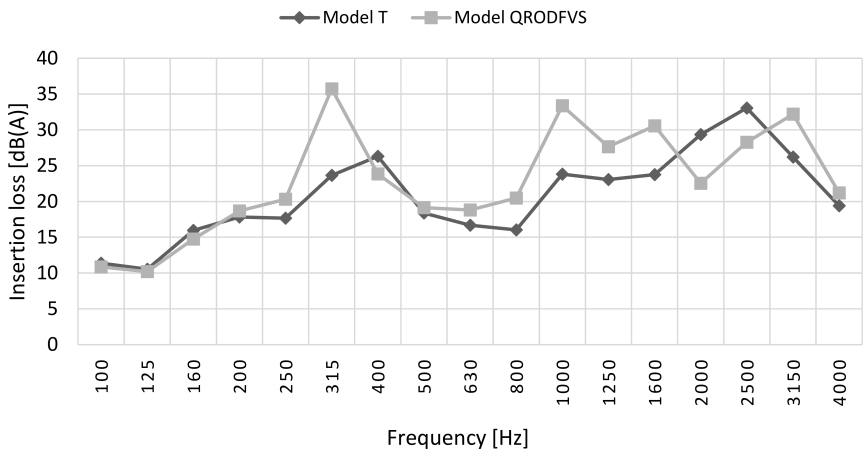

Fig. 9. The Predicted frequency spectra of the barrier insertion loss [dBA] for T-shaped and QRODFVS at the receiver point (20, 1.5).

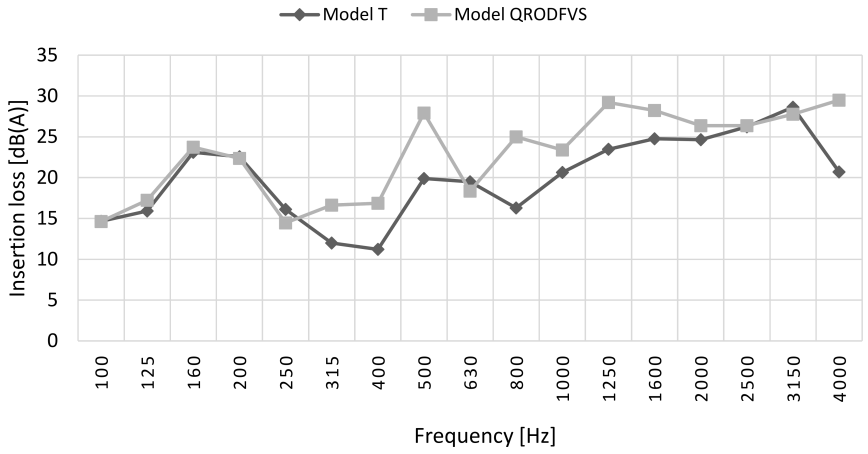

Fig. 10. The Predicted frequency spectra of the barrier insertion loss [dBA] for T-shaped and QRODFVS at the receiver point (20, 3).

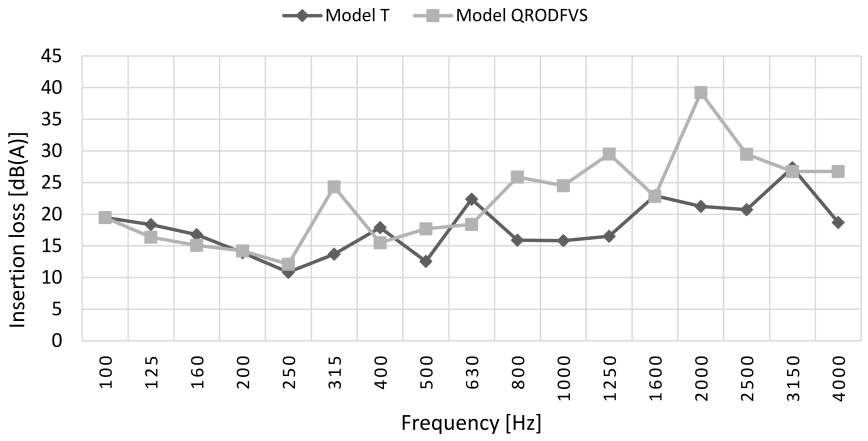

Fig. 11. The Predicted frequency spectra of the barrier insertion loss [dBA] for T-shaped and QRODFVS at the receiver point (20, 4.5).

was different and greater than 250 Hz. Based on the results, it appears that use of the oblique surfaces with a sequence of angles in T-shaped barrier increases the insertion loss at a wide frequency range above 250 Hz significantly. Figures 8–12 shows the peak values of the insertion loss for barrier model of QRODBVS are at 2500, 315, 4000, 2000, 3150 Hz for the heights of 0, 1.5, 3, 4.5, 6 meters, respectively. However, values of the insertion loss of SODBVS model indicated less fluctuation than other barriers at various heights and were appropriate at many frequencies. Therefore, this barrier showed the best performance among designed barriers.

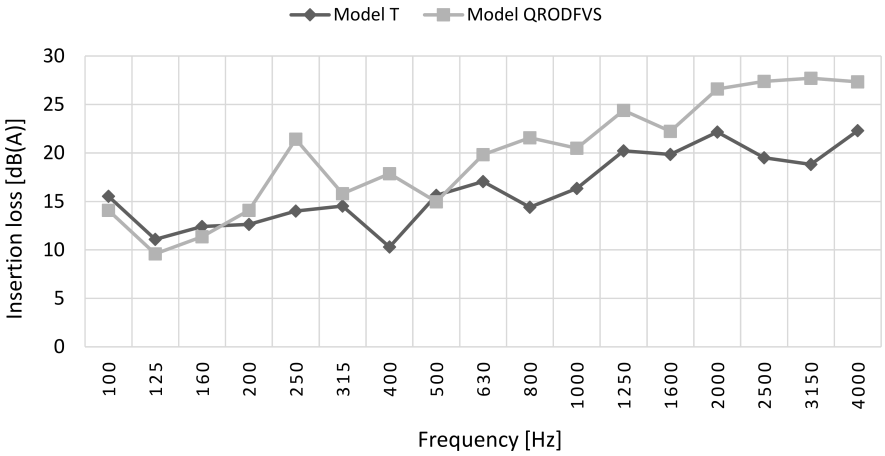

Fig. 12. The Predicted frequency spectra of the barrier insertion loss [dBA] for T-shaped and QRODFVS at the receiver point (20, 6).

Table 3 presents the overall A-weighted insertion loss for QRODFVS model and the reference T-shaped barrier at 20 receiver points. Based on the results, values of the overall A-weighted insertion loss at receiver points 10 (20, 3) and 17 (5, 6) were greatest and least values, respectively. However, the difference values of the insertion loss between ones at receiver points 5 (5, 1.5) and 13 (5, 4.5) were maximum and minimum, respectively. Moreover, Figs 13 and 14 indicate the overall A-weighted values of the insertion loss in barrier models of QRODFVS and T at receiver points, respectively. Values of the improvement in the insertion loss of SODBVS model compared to that of in the reference barrier at receiver points are also depicted in Fig. 15. In all of receiver points, overall A-weighted values of the insertion loss in QRODFVS model were greater than that of the reference T-shaped barrier.

Table 3. The overall A-weighted insertion loss in barrier models of SODBVS and T at receiver points.

Receiver no.	Insertion loss for barrier model T [dBA]	Insertion loss for barrier model QRODFVS [dBA]	Mean difference of insertion loss [dBA]
1	18.3	19.2	+0.9
2	15.9	18.2	+2.3
3	15.0	17.6	+2.6
4	14.7	17.4	+2.7
5	21.0	21.4	+0.4
6	19.6	21.6	+2.0
7	18.2	19.8	+1.6
8	16.2	18.6	+2.4
9	17.1	19.9	+2.8
10	18.3	21.8	+3.5
11	18.2	20.6	+2.4
12	18.0	19.8	+1.8
13	11.5	16.3	+4.8
14	16.6	20.5	+3.9
15	18.4	20.8	+2.4
16	18.0	20.5	+2.5
17	6.7	10.9	+4.2
18	16.0	19.2	+3.2
19	17.5	20.7	+3.2
20	18.0	20.5	+2.5

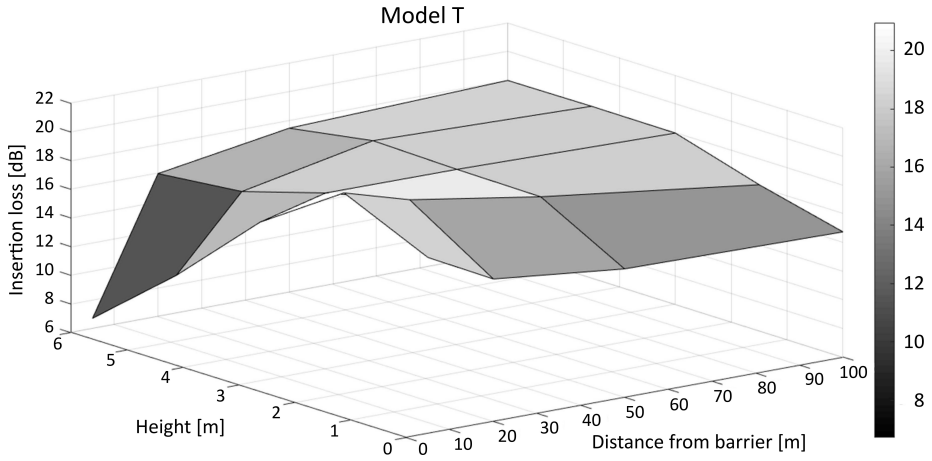

Fig. 13. The overall A-weighted values of insertion loss in reference T-shaped barrier at receiver points.

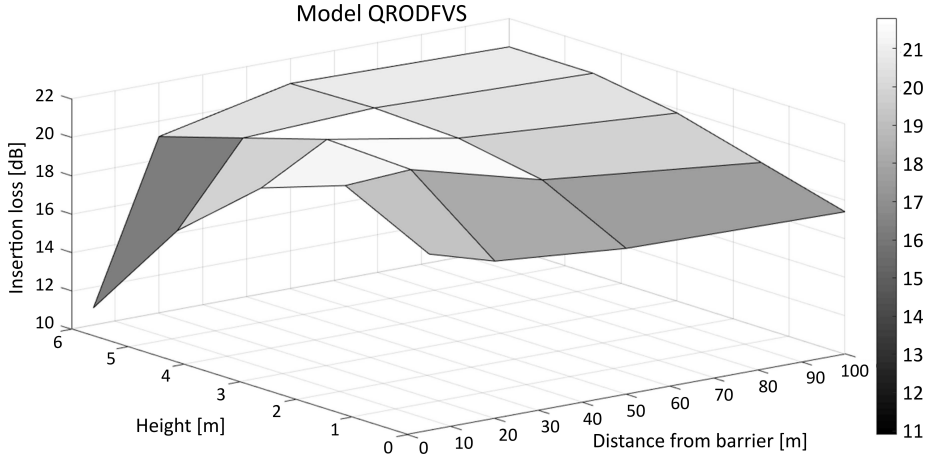

Fig. 14. The overall A-weighted values of insertion loss in barrier model QRODFVS at receiver points.

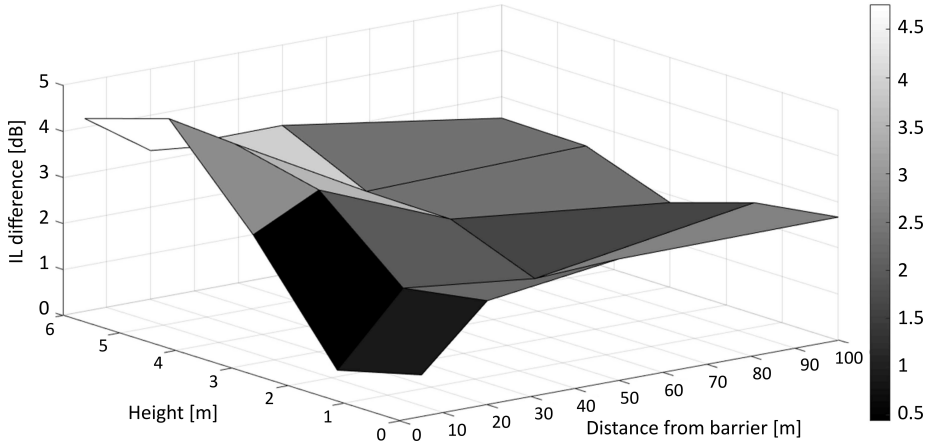

Fig. 15. The values of improvement in insertion loss of barrier model QRODFVS compared to that of in model T at receiver points.

4. Discussion

The performance of designed barriers with various shapes was predicted using 2D boundary element method. Results showed that some changes in the T-shaped barrier were effective. The performance of T-shape noise barriers covered with oblique diffusers improved. The width and height of the barrier stem and the length of the cap were nearly same in all designed barriers. Therefore, values of the insertion loss in the designed barriers have been affected by oblique diffusers on the barrier cap. Of designed

barriers, QRODFVS model indicated the best performance at distance of 20 meters with the various heights. This result can be explained by the constructive and destructive effects of reflected waves based on the boundary geometry and wavelength. The performance of the reference T-shaped barrier was less than that of some designed barriers with oblique diffusers due to the loss of multiple reflection degradation. Constructive effects in some designed barriers with high effective height such as SODF45 and QRODF45 decreased the value of the insertion loss at some heights. In addition, the designed barriers improved, especially the value of the insertion loss at the medium and high frequency. Regarding dimensions and material, this result was predictable. Absorbent materials can be used on rigid surfaces for improvement of the performance at low frequencies. Wu *et al.* introduced a type of profiled absorber which can increase the performance at low frequency (Wu *et al.*, 2001). Moreover, Monazzam, Nassiri (2009) showed that a decrease in the design frequency of the quadratic residue diffusers (QRD) improves the performance at lower frequency (Monazzam, Nassiri, 2009).

In the present study, barriers with backward direction had the superior performance at an angle of 30 and 45 degrees, while the ones with forward direction were better at angles of 45 degree and a sequence of angles. Barriers with forward direction often use the reflection mechanism for reduction of the noise while the dominant mechanism in barriers with backward direction is cancellation. Therefore, the angles of 30 and 45 degrees are optimum values for noise cancellation in designed barriers. As well, quadratic residue oblique diffusers (QROD) had a higher performance at nearly all angles. In general, the quadratic residue oblique diffusers (QROD) created the best values of the insertion loss. However, suitable cancellation happened at an angle of 45 degrees and the sequence of angles for QROD. Quadratic residue diffusers (QRD) showed an appropriate performance in studies performed by other researchers. The results of Monazzam, Nassiri (2009) study demonstrated that use of a QRD with the frequency design of 400 Hz on parallel barrier increases the total performance by 1.8 dBA (Monazzam, Nassiri, 2009). Results of the current study revealed that the design with a sequence of angles provides superior performance because the sequence of angles makes a good condition for the noise cancellation and reflection. Based on these results, at a low height above rigid ground, the value of the insertion loss decreases with the increase of the receiver distance from the barrier, but at higher height, this value enhanced. These findings may be due to the sound refraction. The top surface of T-shaped barriers refracts the sound wave downwards. Additionally, results in Fig. 15 indicate that the QRODFVS model performs better than the reference T-shaped barrier at all receiver points.

5. Conclusion

In general, the result of the current study showed that some designed barriers improved the insertion loss at medium and high frequency. Based on the results, QRODFVS model had the best performance among designed barriers. This design increased the performance of the T-shaped barrier by 0.4 to 4.8 dBA at different distances. In addition, less material is used for construction of this barrier. Therefore, it can be applied effectively to control the noise.

References

1. Abbasi M., Monnazzam M.R., Zakerian S., Yousefzadeh A. (2015), *Effect of wind turbine noise on workers' sleep disorder: a case study of Manjil wind farm in northern Iran*, Fluctuation and Noise Letters, **14**, 2, 15–20.
2. Basner M. *et al.* (2014), *Auditory and non-auditory effects of noise on health*, The Lancet, **383**, 9925, 1325–1332.
3. Baulac M., Defrance J., Jean P. (2008), *Optimisation with genetic algorithm of the acoustic performance of T-shaped noise barriers with a reactive top surface*, Applied Acoustics, **69**, 4, 332–342.
4. Brunner D., Junge M., Rapp P., Bebendorf M., Gaul L. (2010), *Comparison of the fast multipole method with hierarchical matrices for the Helmholtz-BEM*, Computer Modeling in Engineering & Sciences (CMES), **58**, 2, 131–160.
5. EN No: 1793-3 (1998), *Road traffic noise reducing devices – Test method for determining the acoustic performance, Part 3: Normalized traffic noise spectrum*, CEN, Brussels, Belgium.
6. EN No: 1793-4 (2015), *Road traffic noise reducing devices – Test method for determining the acoustic performance – Part 4: Intrinsic characteristics – In situ values of sound diffraction*, CEN, Brussels, Belgium.
7. Fan R., Su Z., Cheng L. (2013), *Modeling, analysis, and validation of an active T-shaped noise barrier*, The Journal of the Acoustical Society of America, **134**, 3, 1990–2003.
8. Fard S.M., Kessissoglou N., Samuels S., Burgess M. (2013), *Numerical study of noise barrier designs*, Proceeding of Acoustics, Victor Harbor, Australia, November 2013.
9. Garai M. (2004), *The new European standard for qualifying added devices*, CD-ROM of 18th ICA Kyoto, http://lib.ioa.ac.cn/ScienceDB/18TH-ICA/pdf/Mo5.F.3.pdf.
10. Garai M., Guidorzi P. (2007), *Using CEN/TS 1793-4 to develop an acoustically effective added device for road traffic noise barriers*, 19th International Congress on Acoustics, Madrid, http://www.sea-acustica.es/WEB_ICA_07/fchrs/papers/env-06-004.pdf.

11. Greiner D., Aznárez J.J., Maeso O., Winter G. (2010), *Single-and multi-objective shape design of Y-noise barriers using evolutionary computation and boundary elements*, Advances in Engineering Software, **41**, 2, 368–378.

12. Halim H., Abdullah R., Ali A.A.A., Nor M.J.M. (2015), *Effectiveness of existing noise barriers: comparison between vegetation, concrete hollow block, and panel concrete*, Procedia Environmental Sciences, **30**, 217–221.

13. Hothersall D., Crombie D., Chandler-Wilde S. (1991), T*he performance of T-profile and associated noise barriers*, Applied Acoustics, **32**, 4, 269–287.

14. Ishizuka T., Fujiwara K. (2004), *Performance of noise barriers with various edge shapes and acoustical conditions*, Applied Acoustics, **65**, 2, 125–141.

15. Khoshakhlagh A.H., Ghasemi M. (2017), *Occupational Noise Exposure and Hearing Impairment among Spinning Workers in Iran*, Iranian Red Crescent Medical Journal, **19**, 5, 1–7.

16. Koussa F., Defrance J., Jean P., Blanc-Benon P. (2013), *Acoustic performance of gabions noise barriers: numerical and experimental approaches*, Applied Acoustics, **74**, 1, 189–197.

17. May D.N., Osman N. (1980), *Highway noise barriers: new shapes*, Journal of Sound and Vibration, **71**, 1, 73–101.

18. McNair E.P. (1995), *Sound barrier with oblique surfaces*, Google Patents.

19. Monazzam M., Lam Y. (2005), *Performance of profiled single noise barriers covered with quadratic residue diffusers*, Applied Acoustics, **66**, 6, 709–730.

20. Monazzam M., Lam Y. (2008), *Performance of T-shape barriers with top surface covered with absorptive quadratic residue diffusers*, Applied Acoustics, **69**, 2, 93–109.

21. Monazzam M., Naderzadeh M., Nassiri P., Fard S. (2010), *Performance of environmental T-shape noise barriers covered with primitive root diffusers*, Archives of Acoustics, **35**, 4, 565–578.

22. Monazzam M., Nassiri P. (2009), *Performance of profiled vertical reflective parallel noise barriers with quadratic residue diffusers*, International Journal of Environmental Research, **3**, 1, 69–84.

23. Naderzadeh M., Monazzam M.R., Nassiri P., Fard S.M.B. (2011), *Application of perforated sheets to improve the efficiency of reactive profiled noise barriers*, Applied Acoustics, **72**, 6, 393–398.

24. Okubo T., Matsumoto T., Yamamoto K., Funahashi O., Nakasaki K. (2010), *Efficiency of edge-modified noise barriers: Intrinsic efficiency determination of practical products and prediction of the diffracted sound field*, Acoustical Science and Technology, **31**, 1, 56–67.

25. Wang Y., Jiao Y., Chen Z. (2018), *Research on the well at the top edge of noise barrier*, Applied Acoustics, **133**, 118–122.

26. Wu T., Cox T.J., Lam Y. (2001), *A profiled structure with improved low frequency absorption*, The Journal of the Acoustical Society of America, **110**, 6, 3064–3070.

27. Yamamoto K. (2015), *Japanese experience to reduce road traffic noise by barriers with noise reducing devices*, 10th European Congress and Exposition on Noise Control Engineering, EuroNoise 2015, 31 May – 3 June, Maastricht, https://www.conforg.fr/euronoise2015/proceedings/data/articles/000606.pdf.